Imperfect gluing bifurcation in a temporal glide-reflection symmetric Taylor–Couette flow

F. Marques
Departament de Física Aplicada, Universitat Politècnica de Catalunya, 08034 Barcelona, Spain

J. M. Lopez[a)]
Department of Mathematics and Statistics, Arizona State University, Tempe, Arizona 85287-1804

V. Iranzo
Departament de Física Aplicada, Universitat Politècnica de Catalunya, 08034 Barcelona, Spain

(Received 15 January 2002; accepted 18 March 2002; published 19 April 2002)

The unfolding due to imperfections of a gluing bifurcation occurring in a periodically forced Taylor–Couette system is numerically analyzed. In the absence of imperfections, a temporal glide-reflection Z_2 symmetry exists, and two global bifurcations occur within a small parameter region: a heteroclinic bifurcation between two saddle two-tori and a gluing bifurcation of three-tori. Due to the presence of imperfections, these two global bifurcations collide, strongly reducing the range of validity of the generic unfolding of the gluing bifurcation. © *2002 American Institute of Physics.* [DOI: 10.1063/1.1476915]

Global bifurcations play a key role as organizing centers in fluid dynamics, especially where multiple states coexist. Their systematic study has generally been limited to theoretical analysis of normal forms and other low-dimensional canonical models, and to experimental investigations. A class of global bifurcations that has been receiving much attention of late is the gluing bifurcation.[1–5] This is a global bifurcation where two symmetrically related time-periodic states simultaneously become homoclinic to an (unstable) saddle state and result in a single symmetric time-periodic state, as a parameter is varied.

In this Letter, we explore the unfolding, due to imperfect symmetry, of a gluing bifurcation in a system with Z_2 symmetry generated by a space-time gliding symmetry, i.e., a half period time translation plus a space reflection. This symmetry has received much attention of late,[6,7] and it is becoming more and more apparent that even systems that do not have this symmetry (in a nontrivial way) in their basic state, have states invariant to it after some local bifurcations have occurred. Many periodically forced systems have a Z_2 space-time symmetry; systems with a space-reflection symmetry which bifurcate to a traveling wave also exhibit this symmetry (e.g., the von Karman wake behind a cylinder, Taylor–Couette flow, and Rayleigh–Bénard convection). The presence of a temporal glide-reflection symmetry strongly affects the dynamics of the system. It may inhibit some bifurcations, typically period doubling;[8] and in many cases rich dynamics associated with homoclinic/heteroclinic behavior is present.

Recent experimental investigations of Taylor–Couette flow in annuli with height-to-gap ratios of order 10 have identified the presence of an imperfect gluing bifurcation.[9,5] The imperfection in the physical experiment is difficult to quantify, and is expected to be high-dimensional. Nevertheless, the abstract dynamical systems theory is not concerned with the precise details of the imperfection, a measure of its magnitude suffices. Recently, we have also found a gluing bifurcation in computed solutions of a temporally forced Taylor–Couette system with aspect ratio 10.[3,4] The temporal forcing aids in the analysis of the problem in that the Z_2 spatial reflection symmetry of the unforced system is replaced by a spatio-temporal glide reflection symmetry which can be broken in a very controlled and simple manner, i.e., by adding a small multiple of the first temporal harmonic of the forcing, this multiple being the small imperfection parameter. Analysis of the experimental results[9,5] indicate that the dynamics associated with the gluing bifurcation are taking place in an axisymmetric [$SO(2)$ invariant] subspace, even though the observations of these dynamics are from solutions with broken $SO(2)$ symmetry. Our computational investigation allows us to trivially isolate the gluing bifurcation from any $SO(2)$ symmetry breaking related dynamics by simply restricting the computations to the axisymmetric subspace. Furthermore, with accurate numerics, we are able to take into account the precise details of the Z_2 symmetry breaking and give quantitative measures of the invariant homoclinic curves in the two parameter bifurcation diagram, as well as estimates of the saddle index and the extent in parameter space (including the symmetry-breaking parameter) over which the gluing dynamics are robust. This level of contact with the abstract dynamical systems theory is possible due to the control that the numerics allows. What is also unique and novel to our study is that in our problem, there are two global bifurcations occurring within a small parameter region, a heteroclinic bifurcation between two saddle two-tori leading to the birth of a symmetric three-torus that undergoes the gluing bifurcation giving two branches of symmetrically related three-tori. The symmetry breaking im-

a)Author to whom correspondence should be addressed. Telephone: (480) 965-8843; fax: (480) 965-0461; electronic mail: lopez@math.asu.edu

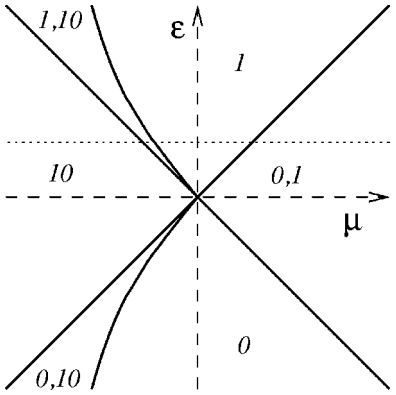

FIG. 1. Bifurcation diagram for the unfolding of the gluing bifurcation.

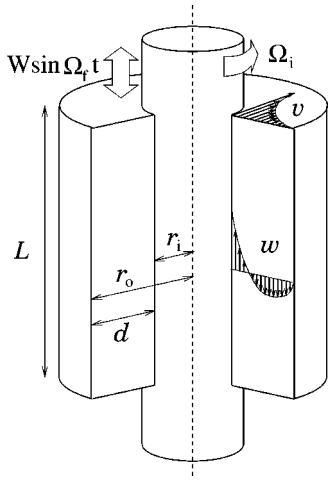

FIG. 2. Schematic of the flow configuration.

perfection provides a strong interaction between these two global bifurcations, altering the canonical unfolding of the gluing bifurcation.

A classification of the possible gluing bifurcation scenarios was obtained and analyzed in Refs. 10–12, and a recent discussion of the unfolding due to imperfections is presented in Ref. 13. The unfolding of the bifurcation is described by two parameters, μ (related to the Reynolds number in our problem) and ϵ, the imperfection parameter. A schematic of the bifurcation diagram is displayed in Fig. 1. The horizontal axis ($\epsilon=0$) corresponds to perfect Z_2 symmetry; for $\mu<0$ a symmetric limit cycle labeled 10 collides with the saddle at $\mu=0$, forming a homoclinic curve with two closed loops, and for $\mu>0$ splits into two asymmetric limit cycles, labeled 0 and 1 which are related by the symmetry. For $\epsilon\neq 0$, the gluing bifurcation splits into two separate single loop homoclinic bifurcations, corresponding to the solid straight lines in Fig. 1. These lines delimit four regions. Two of them are extensions of the symmetric case, and contain the single limit cycle 10 or the two limit cycles 1 and 0 which are no longer symmetrically related. In the two additional regions only one limit cycle exists, 1 and 0, respectively. There exist two additional cusp-shaped regions, where two limit cycles coexist, 1 and 10, and 0 and 10, respectively. The three limit cycles (0,1,10) involved in the gluing bifurcation in the symmetric case give rise to three branches of limit cycles that disappear in generic homoclinic bifurcations (collision of the limit cycle with a saddle) when $\epsilon\neq 0$, corresponding to the solid lines in Fig. 1. The dotted line in the figure corresponds to a typical path in the presence of a fixed imperfection ($\epsilon\neq 0$).

Other gluing bifurcation scenarios are possible; these were obtained and analyzed in Refs. 10–12. They differ in the size of and the dynamics in the cusp regions. Above we described the simplest scenario that happens to correspond to our problem. This same scenario has been recently observed experimentally in a similar unforced Taylor–Couette flow.[5]

The model problem we consider is the flow between two coaxial finite cylinders with stationary top and bottom endwalls. The outer cylinder is also stationary while the inner cylinder rotates at constant angular velocity Ω_i and oscillates in the axial direction with velocity $W\sin\Omega_f t$. Its radius is r_i, the radius of the outer cylinder is r_o, and their length is L; the annular gap between the cylinders is $d=r_o-r_i$ (see Fig. 2). These parameters are combined to give the following nondimensional governing parameters: the radius ratio $e=r_i/r_o$, the length to gap ratio $\Lambda=L/d$, the Couette flow Reynolds number $Ri=dr_i\Omega_i/\nu$, the axial Reynolds number $Ra=dW/\nu$, and the nondimensional forcing frequency $\omega_f=d^2\Omega_f/\nu$, where ν is the kinematic viscosity of the fluid. The basic flow is time-periodic with period $T_f=2\pi/\omega_f$ and synchronous with the forcing, and it is independent of the azimuthal coordinate.

The incompressible Navier–Stokes equations governing this problem are invariant to two symmetry groups. One corresponds to rotations around the common axis of the cylinders, $SO(2)$. The other, a temporal glide-reflection Z_2, is generated by the discrete symmetry S, involving time and the axial coordinate; it is a reflection about the midplane orthogonal to the axis with a simultaneous time translation of a half forcing period, satisfying $S^2=I$. In this study we solve the system in an axisymmetric subspace invariant to $SO(2)$, and therefore the only relevant symmetry group is Z_2. The symmetries $SO(2)$ and Z_2 for this problem commute.

The temporal glide reflection produces a convoluted bifurcation scenario in this flow, comprising of a gluing of three-tori ($\mathbb{T}^3$) and homoclinic and heteroclinic dynamics.[3,4] This gluing bifurcation is the organizing center of the dynamics and is responsible for spontaneous symmetry breaking in this problem.

We consider an imperfection of the harmonic character of the oscillation of the inner cylinder. It is very difficult to obtain a pure harmonic oscillation in an experiment, and with any deviation from harmonicity, S ceases to be a symmetry of the system. The nonharmonic axial oscillations have the form $W(\sin\Omega_f t+\epsilon\sin 2\Omega_f t)$, where ϵ is a measure of the imperfection.

The axisymmetric Navier–Stokes equations have been solved with the spectral scheme described in Ref. 4. By varying only Ri and ϵ and keeping all other parameters fixed ($\Lambda=10$, $e=0.905$, $Ra=80$, $\omega_f=30$), we located a range ($Ri\in[280.89,281.26]$ for $\epsilon=0$) where stable $\mathbb{T}^3$ solutions exist. The identification of such solutions was significantly

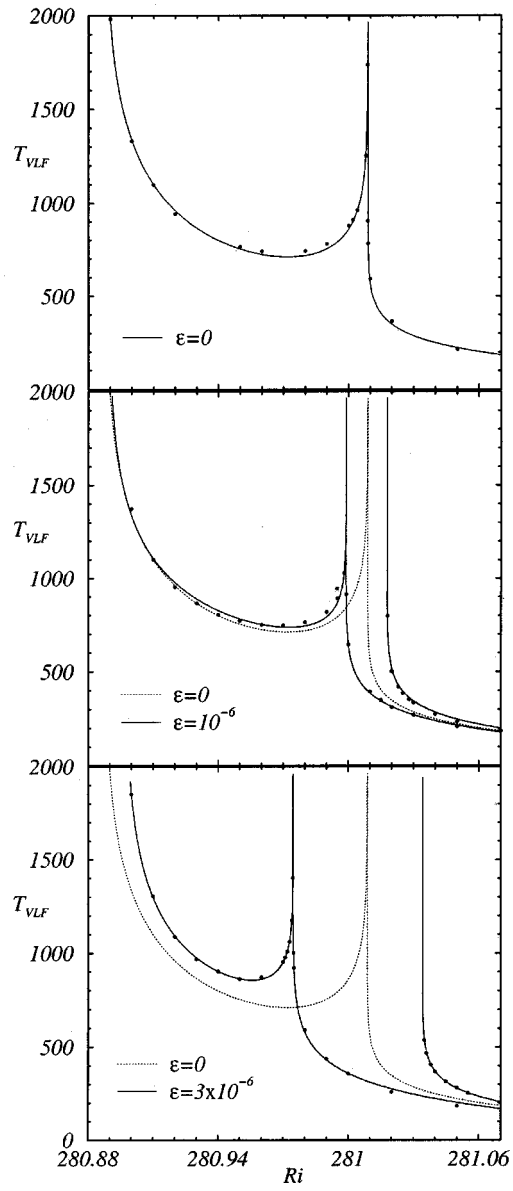

FIG. 3. Variation of $T_{\mathrm{VLF}}=2\pi/\omega_{\mathrm{VLF}}$ with Ri for ϵ as indicated. Symbols correspond to computed cases and lines are logarithmic fits.

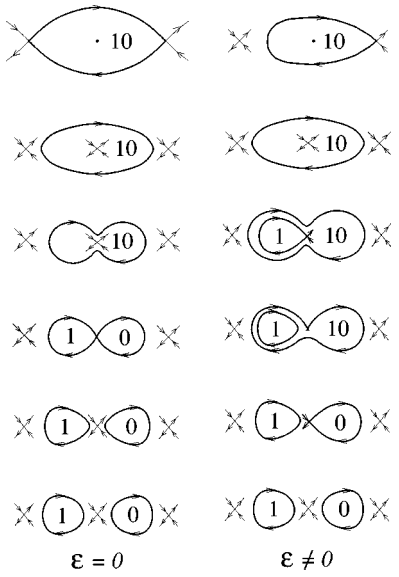

FIG. 4. Schematic of the bifurcation sequence for the $\mathbb{T}^3$ solutions. In this schematic, $\mathbb{T}^2$ are represented as fixed points and $\mathbb{T}^3$ as cycles.

helped by the use of a global Poincaré map for the system (i.e., strobing at the forcing frequency ω_f). The three tori solutions have three incommensurate frequencies: the forcing frequency, $\omega_f=30$, a second frequency at $\omega_s\approx 5.2$, and a very low frequency ω_{VLF} which is three orders of magnitude smaller than ω_s.

Over the range of Ri and ϵ where $\mathbb{T}^3$ solutions exist, $T_{\mathrm{VLF}}=2\pi/\omega_{\mathrm{VLF}}$ experiences dramatic changes, as shown in Fig. 3 for $\epsilon=0$. This figure indicates that there are two Ri values where T_{VLF} becomes unbounded. The solid curves are best fits of the form $T_{\mathrm{VLF}}\sim\lambda^{-1}\ln(1/|Ri-Ri_{crit}|)+a$, the asymptotic behavior of the period close to a homoclinic connection.[14] The logarithmic fits give the critical Ri for the two infinite-period bifurcations at $\epsilon=0$, $Ri_{he}=280.88736$ and $Ri_{gl}=281.00885$. The factors λ are the eigenvalues corresponding to the unstable direction of the hyperbolic fixed points (saddle $\mathbb{T}^2$). The values obtained are $\lambda_{he}=2.43\times10^{-3}$ and $\lambda_{gl}=1.047\times10^{-2}$. For $\epsilon\neq=0$, the $T_{\mathrm{VLF}}\to\infty$ gluing bifurcation splits into three distinct homoclinic bifurcations as shown in Fig. 3. Note that the range in Ri where the 1 and 10 $\mathbb{T}^3$ branches coexist (i.e., the width of the cusp region in Fig. 1) is very narrow for the imperfections considered and so the two distinct homoclinic bifurcations appear to coincide on the scale of the graphics in Fig. 3. Specifically, for $\epsilon=10^{-6}$, the width in Ri of the cusp coexistence region is 5.44×10^{-5} and for $\epsilon=3\times10^{-6}$ it is 2.40×10^{-4}. This behavior agrees with the unfolding of a gluing bifurcation, depicted in Fig. 1. The periods of the $\mathbb{T}^3$ follow the same asymptotic logarithmic expression as for $\epsilon=0$, showing that the $\mathbb{T}^3$ for $\epsilon\neq0$ disappear in a collision with a saddle $\mathbb{T}^2$ (a generic homoclinic bifurcation).

Figure 4 illustrates schematically the sequence of bifurcations on the $\mathbb{T}^3$ branches; $\mathbb{T}^3$ are depicted as limit cycles and $\mathbb{T}^2$ as fixed points. This analogy works since the two suppressed frequencies, ω_f and ω_s, are almost constant (in fact, ω_f is constant), over the range of Ri and ϵ of interest, and they do not play an essential role in the dynamics near the bifurcation points. The first column in the figure corresponds to the Z_2-symmetric case ($\epsilon=0$), reported in Refs. 3 and 4. The infinite-period bifurcation at Ri_{he} corresponds to a heteroclinic loop connecting two saddle $\mathbb{T}^2$ that are related to each other via the temporal glide-reflection symmetry. The $\mathbb{T}^3$ that emerges for higher Ri values (labeled 10) is invariant, and undergoes a gluing bifurcation at Ri_{gl}. For larger Ri values two asymmetric $\mathbb{T}^3$ exist, 1 and 0. These $\mathbb{T}^3$ solutions become unstable beyond $Ri=281.26$, and the system evolves towards a $\mathbb{T}^2$ branch described in Refs. 3 and 4. The second column in Fig. 4 is a schematic of the imperfect ($\epsilon=0$) case. Both the gluing and the heteroclinic bifurcations become standard homoclinic bifurcations, and we have three different branches (10, 0, 1) that overlap for different values of Ri in agreement with the theoretical description in Fig. 1. The equations of the straight lines and the cusp curve in this

figure can be obtained from the numerical simulations. As a result we have accurately obtained the location of the gluing bifurcation, $R_{gl}=281.01$, the unstable eigenvalue of the saddle at the gluing point, $\lambda_1=1.047\times10^{-2}$ and the saddle index (the ratio between the real part of the leading negative eigenvalue and the positive eigenvalue λ_1), $\delta=-\mathrm{Real}(\lambda_2)/\lambda_1=1.083>1$.

For ϵ sufficiently small, our numerical simulations produce dynamics precisely in accord with the dynamical systems theory for the unfolding of a gluing bifurcation: three different branches of $\mathbb{T}^3$ exist, and they appear in homoclinic bifurcations close to the gluing point. But, for our particular problem, the branch of symmetric $\mathbb{T}^3$ (10) undergoes a closeby (at lower Reynolds number) heteroclinic global bifurcation, and when ϵ increases, the two global bifurcations at either end of this branch collide and the $\mathbb{T}^3$ branch labeled 10 disappears (at $\epsilon\approx5\times10^{-6}$ and $Ri\approx280.93$). This collision of global bifurcations (in this case a collision of two homoclinic bifurcations) alters the bifurcation diagram, dramatically reducing the parameter range of validity of the standard unfolding of the gluing bifurcation. The two remaining $\mathbb{T}^3$ branches, labeled 0 and 1, become unstable at higher Ri; and with increasing ϵ, the homoclinic bifurcation points where they are born move apart, one to smaller and the other to larger Ri, as shown in Fig. 3. Therefore, the parameter range of existence of the asymmetric $\mathbb{T}^3$ labeled 0 shrinks until it disappears at about $\epsilon\approx10^{-5}$. Only one of the $\mathbb{T}^3$ branches (1) is robust enough to be observable in a significant window of parameter space.

The periodically forced annular flow has revealed some very interesting and novel dynamics associated with global bifurcations of $\mathbb{T}^3$. Apart from the unfolding of a gluing bifurcation, which is an area that is just being explored in several different extended systems, we have also identified a nearby heteroclinic bifurcation, that in the presence of imperfect Z_2 symmetry, acts to limit the range of validity of the generic unfolding of the gluing by a collision of homoclinic bifurcations. Although in our system the associated dynamics take place over a quite small range of Reynolds numbers, we expect based on trends with others features in Taylor–Couette flow, that in annuli with wider gaps and smaller aspect ratios, the global bifurcations should occur over a more extensive range of Reynolds numbers. Nevertheless, this particular system has presented a new nonlinear dynamics, the interaction and collision between global bifurcations. To our understanding, this has not been previously studied and warrants further experimental, numerical, and theoretical investigations. An implication of the presence of nearby global dynamics interacting with the imperfect gluing bifurcation is that the theoretical picture of the unfolding is completely changed. So, in an experiment with even extremely small levels of imperfection, complex spatio-temporal dynamics can be present that are not obviously associated with the underlying gluing bifurcation (e.g., in our example problem for $\epsilon=10^{-4}$ there is only one branch of $\mathbb{T}^3$, the 1 branch, that is not symmetric and does not undergo any homoclinic bifurcation at this ϵ), and their origin would be difficult to reconcile.

ACKNOWLEDGMENTS

This work was supported by NSF Grants No. INT-9732637 and No. CTS-9908599 (USA) and DGICYT Grant No. BFM2001-2350 (Spain).

[1] S. M. Cox, "2-dimensional flow of a viscous-fluid in a channel with porous walls," J. Fluid Mech. **227**, 1 (1991).
[2] D. Ambruster, B. Nicolaenko, N. Smaoui, and P. Chossat, "Symmetries and dynamics for 2-D Navier–Stokes flow," Physica D **95**, 81 (1996).
[3] J. M. Lopez and F. Marques, "Dynamics of 3-tori in a periodically forced Navier–Stokes flow," Phys. Rev. Lett. **85**, 972 (2000).
[4] F. Marques, J. M. Lopez, and J. Shen, "A periodically forced flow displaying symmetry breaking via a three-tori gluing bifurcation and two-tori resonances," Physica D **156**, 81 (2001).
[5] J. Abshagen, G. Pfister, and T. Mullin, "Gluing bifurcations in a dynamically complicated extended flow," Phys. Rev. Lett. **87**, 224501 (2001).
[6] J. S. W. Lamb and I. Melbourne, "Bifurcation from periodic solutions with spatiotemporal symmetry," in *Pattern Formation in Continuous and Coupled Systems*, Vol. 115 of *IMA Volumes in Mathematics and its Applications*, edited by M. Golubitsky, D. Luss, and S. Strogatz (Springer, New York, 1999), p. 175.
[7] J. S. W. Lamb, I. Melbourne, and C. Wulff, "Bifurcation from periodic and relative periodic solutions in equivariant dynamical systems," in *Equadiff 99, International Conference on Differential Equations*, edited by B. Fiedler *et al.* (World Scientific, Singapore, 2000), p. 175.
[8] J. W. Swift and K. Wiesenfeld, "Suppression of period doubling in symmetric systems," Phys. Rev. Lett. **52**, 705 (1984).
[9] J. von Stamm, U. Gerdts, T. Buzug, and G. Pfister, "Symmetry breaking and period doubling on a torus in the VLF regime in Taylor–Couette flow," Phys. Rev. E **54**, 4938 (1996).
[10] D. V. Turaev, "Bifurcations of two-dimensional dynamical systems close to a system with two separatrix loops," Russ. Math. Surveys **40**, 243 (1985).
[11] D. V. Turaev and L. P. Shil'nikov, "On bifurcations of a homoclinic 'figure eight' for a saddle with a negative saddle value," Sov. Math. Dokl. **34**, 397 (1987).
[12] J. M. Gambaudo, P. Glendinning, and C. Tresser, "Stable cycles with complicated structure," in *Instabilities and Nonequilibrium Structures*, Mathematics and its Applications, edited by E. Tirapegui and D. Villarroel (Reidel, Dordrecht, 1987), p. 41.
[13] P. Glendinning, J. Abshagen, and T. Mullin, "Imperfect homoclinic bifurcations," Phys. Rev. E **64**, 036208 (2001).
[14] P. Gaspard, "Measurement of the instability rate of a far-from-equilibrium steady state at an infinite period bifurcation," J. Phys. Chem. **94**, 1 (1990).